Distributed Fibre Optic Sensing for Monitoring Reinforced Concrete Piles

C. Kechavarzi[1], L. Pelecanos[2], N. de Battista[3], and K. Soga[4]

[1,3]*University of Cambridge, Department of Engineering, Centre for Smart Infrastructure and Construction (CSIC),*
Trumpington Street, Cambridge CB2 1PZ, United Kingdom
[2]*University of Bath, Department of Architecture and Civil Engineering, Claverton Down, Bath BA2 7AY, United Kingdom*
University of California, Berkeley, Department of Civil and Environmental Engineering,
Berkeley, California 94720-1710, USA
E-mail: ck209@cam.ac.uk

ABSTRACT: Distributed fibre optic sensing (DFOS) presents several advantages over traditional point sensors, for measuring strain and temperature in civil and geotechnical infrastructure. DFOS techniques use light transmitted through an optical fibre to enable measurements to be taken all along an embedded or surface-mounted fibre optic cable, which can be up to several kilometres long. This makes DFOS particularly useful for monitoring linear structures and to detect the potential existence of any anomalies which are usually unpredictable. Hence, DFOS has gained in popularity for monitoring reinforced concrete piles, especially during pile testing.

The spatially continuous strain data from DFOS provide detailed information about load transfer along the pile but can also be used to calculate vertical displacements and shaft friction through numerical integration and differentiation, which are useful for validating relevant performance-based numerical models. This paper introduces the methodology and illustrates these advantages through an example obtained from an instrumented pile load test in London. While it synthesises a number of lessons learned in the application of DFOS for pile testing, it also supports the case for routine long-term monitoring of working piles.

KEYWORDS: Distributed fibre optic sensing, Pile load test, Strain, Shaft friction, Monitoring

1. INTRODUCTION

Pile load tests are required and specified when soil conditions, load levels, pile type or installation method are such that there is insufficient comparable experience to provide necessary confidence in the design (Eurocode 7, section 7.5; BS EN 1997-1:2004). The growing use of larger piles, as well the development of new piling technology, have resulted in increased uncertainty over existing design methodologies, which have become difficult to verify against past experience and scarce field data (Soga, 2014, Soga et al., 2015). Hence, design development and validation for such piles rely increasingly on the outcome of pile load tests.

Static load tests are the most accurate method for determining pile load capacities. In the UK, the maintained static vertical load test, where load increments are applied when the rate of induced settlement is below a specified criteria, is most frequently used (Federation of Piling Specialists 2006). The pile is commonly loaded up to the design verification load (DVL) before unloading and applying subsequent load cycles to specified values above the DVL, typically 1.0 or 1.5 times the specified working load (SWL). The load testing methods for maintained load tests in compression comprise reaction piles, Kentledge and bi-directional load cell methods.

While full-scale testing of pile foundations is a well-established technique for design validation, it also provides an opportunity for continuous improvement in pile design and construction practices (Federation of Piling Specialists 2006). Hence, although pile load tests are expensive to implement, they can add value to a structure and, in large projects, lead to significant cost savings through less conservative design. This value, however, is derived from the collection and interpretation of suitable and reliable data. Conventional instrumentation for axially loaded piles commonly includes displacement transducers to measure vertical deflection at the top of the pile, load cells to measure the applied load, embedded vibrating wire strain gauges (VWSG) or sister bars for strain measurements and retrievable or embedded extensometers for relative displacement measurements within the pile.

More recently, however, distributed fibre optic sensing (DFOS) based on Brillouin scattering for strain measurements, has been developed as a viable alternative to strain gauges and extensometers. DFOS has promising advantages over discrete point sensors because it provides a high spatial density of data, where thousands of data points can be obtained along the length of the pile under test. This removes the uncertainty about point sensor performance and potential localised effects affecting sensor output. Conversely, DFOS can pinpoint these localised artefacts, which might be important for the assessment of the pile performance, at any location along the pile's whole depth, by providing an overall picture of strain development under load. DFOS also presents specific practical advantages because the measurements are made over a single fibre optic (FO) cable which is easy to install and because of the very low failure rate of such sensors once installed, since they are not affected by corrosion or water ingress.

The concept of using DFOS for instrumenting cast-in-situ concrete piles in the UK was pioneered by the University of Cambridge over a decade ago (Klar et al., 2006) and implemented in both load test and working piles (Bennett et al, 2006; Mohamad, 2008). Since then the Cambridge Centre for Smart Infrastructure and Construction (CSIC) and its various industry partners have further developed and standardised the installation and testing procedures of DFOS through the instrumentation of numerous axially loaded cast-in-situ concrete piles (Ouyang et al., 2015, de Battista et al., 2016a; Pelecanos et al., 2017 and 2018), including continuous flight auger (CFA) (de Battista et al., 2016b) and tension piles (Pelecanos et al., 2016). CSIC has recently contributed to the development of specifications for the use of DFOS for pile instrumentation which is now included in the third edition of the Institution of Civil Engineers (ICE) Specifications for Piling and Embedded Retaining Walls (2016), the reference document for piling works in the UK. CSIC has also published a specialist best practice guide for the use of DFOS for monitoring general civil infrastructure (Kechavarzi et al., 2016).

This paper presents an overview of the DFOS technology and its implementation in cast-in-situ test piles, as well as the relevant geotechnical information that can be derived with spatially continuous strain data, through a case study.

2. DISTRIBUTED FIBRE OPTIC SENSING (DFOS)

2.1 Measuring principle of DFOS based on Brillouin scattering

The DFOS techniques that have commonly been used on pile load tests are standard Brillouin Optical Time Domain Reflectometry (BOTDR) or Analysis (BOTDA), which are based on the principle of spontaneous and stimulated Brillouin scattering, respectively. They rely on the fact that light travelling in an optical fibre will be

fractionally backscattered due to small refractive index or density fluctuations. The spectrum of the backscattered light is characterised by well known features, including the Brillouin frequency peaks, as shown in Figure 1. Brillouin scattering is due to the interaction of the incident light wave photons with propagating density waves or acoustic phonons resulting in a shift in photon energy. The scattering is inelastic and the photons may lose or gain energy (Stokes and anti-Stokes processes) and create or absorb phonons. This results in a shift in the frequency of the scattered light wave (Figure 1), called Brillouin frequency shift.
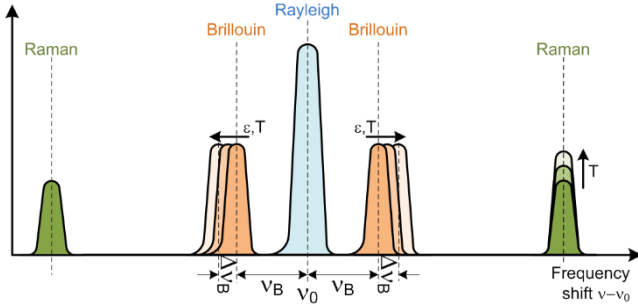

Figure 1 Components of the backscattered light spectrum in an optical fibre

As long as the amount of light that is scattered due these acoustic vibrations generated by the thermal agitation is too small to excite further fluctuations in the density of the medium, the process is known as spontaneous Brillouin scattering (Bao and Chen, 2011). This is used in BOTDR where a pulsed laser signal (pump wave) is launched in a single-ended optical fibre to generate spontaneous scattering.

Conversely, larger numbers of scattered photons can lead to the effect known as stimulated Brillouin scattering, where the medium is said to be a Brillouin generator (Bao and Chen, 2011). As is used in BOTDA, stimulated Brillouin scattering can be generated by launching an additional continuous, counter-propagating probe wave into the opposite end of a double-ended optical fibre.

The Brillouin frequency shift from the incident light wave frequency at a wavelength of 1550 nm is around 10-11 GHz. The value of the Brillouin peak frequency, v_B, is proportional to the velocity of the acoustic phonons and phase refractive index, which in turn depend on local temperature and material density. Hence, for the temperature range encountered in most geotechnical applications, this frequency varies linearly with changes in longitudinal strain and temperature in the fibre core / cladding so that (Horiguchi et al., 1989):

$$\Delta v_{BS} = C_\varepsilon \Delta \varepsilon_a + C_T \Delta T \qquad (1)$$

where Δv_{BS} is the change in Brillouin frequency due to a simultaneous change in axial strain, $\Delta \varepsilon_a$, and in temperature, ΔT. C_ε and C_T are referred to as the strain and the temperature coefficient of the Brillouin frequency shift, respectively.

These coefficients essentially depend on the material properties and geometry of the optical fibre. Hence, for standard telecommunication single mode fibres, and at the operating wavelength of 1550 nm, C_ε and C_T will have values close to 500 MHz/% and 1 MHz/°C, respectively. Nonetheless, it is important to note that, in a strain cable, if the strain is only partially transferred to the optical fibre through the cable coatings, the value of the strain coefficient will be lower than 500 MHz/%.

With both BOTDR and BOTDA, the Brillouin spectrum generated at a given location along the optical fibre is reconstructed using a spectrum analyser by measuring the Brillouin gain while changing the frequency of the pump wave in successive increments. The distance from the position where the pulsed light is launched to the position where scattered light is generated and the spectrum reconstructed, can be determined from a time-domain analysis by measuring the propagation times of the light pulse traveling in the fibre. This results in a three-dimensional Brillouin gain spectrum, as shown in Figure 2, where the Brillouin peak frequency, v_B, needed to calculate strain and / or temperature (Eq. 1) is obtained at each position along the optical fibre by fitting the spectrum with an appropriate function such as a Lorentzian curve (Zhang and Wu, 2008). This provides strain and / or temperature data points along the optical fibre, the spatial distribution of which depends on spectrum analyser specifications.
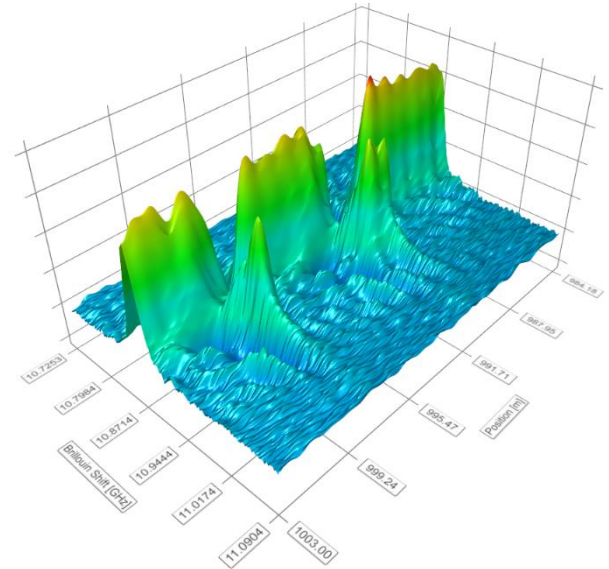

Figure 2 Three-dimensional Brillouin gain spectrum measured by Brillouin Optical Frequency Domain Analysis (fibrisTerre Systems GmbH)

Figure 2 showing a frequency increase in two fibre sections of one and two meters, caused by a 55°C change in temperature.

2.2 Temperature compensation

In practice, since the influence of temperature and strain on the Brillouin frequency is coupled (Eq. 1), it is necessary to distinguish between these two effects. A common solution is to use a separate temperature compensation cable placed adjacent to the strain cable, or a single cable containing both a fibre used to measure strain and one to measure temperature. In both cable types, the fibre used to measure temperature is contained in a loose tube that is filled with either gel or air. In this loose tube construction, the optical fibre is isolated from mechanical strain effects and the Brillouin frequency is only affected by temperature effects. These are the temperature effect on the Brillouin frequency, $C_T \Delta T$, coupled with the strain, $\alpha \Delta T$, generated by the thermal expansion of the optical fibre in the loose tube, α being the thermal expansion coefficient of the fibre. These effects can be lumped into a single coefficient, $\beta = C_T + \alpha$ so that, for a loose tube cable:

$$\Delta v_{BT} = \beta \Delta T \qquad (2)$$

where, Δv_{BT}, is the change in Brillouin frequency measured in the fibre used for temperature compensation. β is obtained through temperature calibration of the cable.

Hence, with this method, temperature changes, ΔT, can be measured independently and substituted into Eq. 1 to calculate strain changes solely due to stress generated by load or thermal expansion of the structure under study. A practical challenge when using distinct strain and temperature cables, is to record their physical position on

the structure accurately so that the temperature measured at a given location can be used to compensate the effect on the strain cable at the same location.

2.3 System specifications

Parameters of importance for the engineer specifying DFOS for a pile load test (or any other application) are the measurement accuracy, resolution and precision (repeatability) of the system, the spatial and sampling resolutions, the distance range, the measurement or acquisition time, and the dynamic range or optical budget. These will mainly depend on the spectrum analyser but also on the type of cables used and the quality of the installation.

The accuracy is the deviation between the measured value and the measurand true value. For a given analyser, it is dependent on the accuracy of the calibration of the FO cables used. The measurement resolution is the standard deviation of the noise over a series of repeated measurements, while the precision of the measurement is double this standard deviation. The precision is often referred to as the repeatability.

The spatial resolution is the smallest distance over which a change in strain or temperature can be measured with full accuracy. This is an important characteristic of the system and is mainly dependent on the duration of the transmitted pulse of light. The spatial resolution of most standard commercial BOTDR and BOTDA is currently limited to between 0.5 and 1 m. However data points can be sampled at spatial intervals much lower than the spatial resolution (as low as a few centimetres) depending on the time interval between two consecutive sampling points digitised by the instrument. This so called sampling resolution or sampling interval is not a physical parameter and does not improve the spatial resolution, but the data points are moving averages that can contribute to the spatial accuracy and the detection of localised events such as sharp strain or temperature transitions.

The distance range is the maximum distance over which a measurement can be made at a specified spatial resolution and with a specified measurement precision. This distance can reach tens of kilometres. The acquisition time is the amount of time required for one measurement. With standard analysers, acquisition times of several minutes are necessary to achieve measurements with meaningful precisions.

The optical budget is the maximum amount of optical loss permissible in order to achieve a measurement at the specified distance and with the specified spatial and measurement resolution.

It is important to note that the overall performance of the system will be controlled by the interdependence of the above parameters. For example the decrease in resolution and precision over long-range measurements due to higher optical losses and a decrease in signal to noise ratio will need to be counterbalanced by increasing the acquisition time (averaging) as well as the pulse widths (i.e. lower the spatial resolutions).

Nevertheless, this is unlikely to play a significant role with pile load tests where fibre lengths are in the order of several hundreds of meters, as long as optical losses following installation are below the chosen optical budget. In this case, the optimum strain precision of around ±20 με for a standard BOTDR and ±5 με for a BOTDA is likely to be achievable over the length of the installation, with the highest spatial resolution of 0.5 – 1 m and single measurement times not exceeding 5 – 10 minutes.

These specifications have important implications for the design of the measurement system or that of the load test. For example, each load step would have to be maintained by at least the length of time that it takes to obtain two measurements, in order to ensure that at least one measurement is acquired at that load. It is also vital to have some prior knowledge of the magnitude of the minimum strain that needs to be measured and to ensure that it is significantly higher than the measurement precision. For pile load tests, Figure 3 shows how an initial estimate of the maximum axial strain can be obtained with prior knowledge of the applied force and pile diameter. This is done

by dividing the applied force, F, by the axial rigidity, EA, where E is the modulus of elasticity and A is the pile cross sectional area.
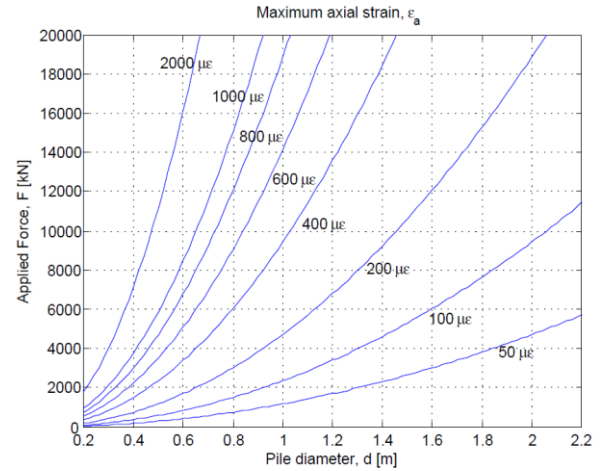

Figure 3 Maximum axial strain expected to be developed at the top of a pile during a load test, as a function of the applied load and pile diameter

2.4 DFOS cables

For a FO cable to qualify as a strain cable, the strain applied to the jacket needs to be transferred to the fibre core by limiting the potential slippage between the different protective coatings. This complicates the development of such cables, which need appropriate protection against harsh conditions and handling during installation.

Strain cables should be calibrated to ensure the uniformity of the strain transfer along their length, ensure that strain is transferred linearly so that Eq. 1 applies, and to determine the value of the strain coefficient C_ε. This is done by applying a known amount of strain to a given length of cable, while measuring the peak Brillouin frequency under constant temperature, so that $C_T \Delta T = 0$ in Eq. 1. Figure 4a shows the linear relationship between frequency and strain changes, obtained at one measuring point for the strain cable used in the case study presented below. This cable, manufactured by Fujikura Ltd (Japan), is a flat ribbon cable made of nylon with four central optical fibres and two lateral steel reinforcement wires.

Conversely, cables used for temperature compensation require that the strain transfer to the fibre is negligible. These usually consist of gel or air filled loose tube configurations to allow slippage and free expansion or contraction of the fibre. These cables can be calibrated in temperature controlled thermal water baths, or in environmental or climatic chambers, in order to determine the coefficient β in Eq. 2. The cable can be tested over the temperature range of interest. Figure 4b shows the linear relationship between frequency and temperature changes obtained at one measuring point for a steel reinforced gel-filled loose tube temperature cable manufactured by Brugg Kabel AG (Switzerland), using a water bath over the temperature range of 10 – 100°C.

3. METHOD OF INSTALLATION

As mentioned in Section 2.3, the accuracy, resolution and precision of the data acquired from the DFOS system is dependent on the quality of the sensor cable installation. Therefore the careful design, installation and testing of the system should be given due importance.

3.1 Sensor design and preparation

Starting from the reinforcement drawings of the test pile, the first step is to design the layout of the FO sensing cables (temperature and

strain pair) within the pile. These are installed as one or more loops, to be attached on opposite sides of the pile cage/s, looping at the bottom of the pile, and with both ends exiting the pile head. In piles with a diameter up to 0.9 m, it is common to use one or two loops of FO cables (i.e. measuring along two or four sides of the pile, respectively). Larger diameter piles tend to be instrumented with more sensor cable loops. The sensor cables need to be long enough to extend down the full length of the pile while leaving at least 3 to 5 m of cable exiting the pile head, so that they can be connected together in series to form a complete FO circuit, after the pile has been constructed.
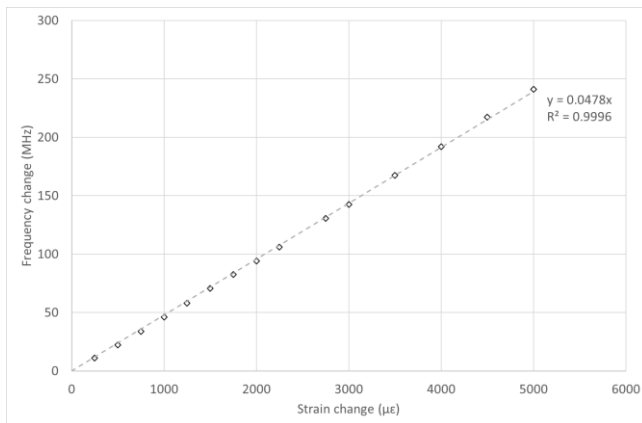
(a)
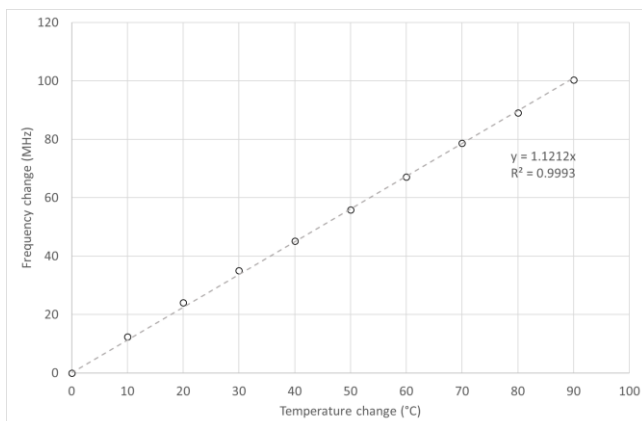
(b)

Figure 4 (a) Strain coefficient calibration at constant temperature of 20ºC and (b) Temperature calibration using a water bath

After the system is designed and cables lengths determined, the cables are then prepared off-site, where they are cut to the correct length and coiled on reels. Each end of the cables is fusion spliced to a FO connector which enables the cable to be tested and also facilitates the connection of the individual cables together after they are installed in the pile.

3.2 Sensor installation

The installation of the cables on site starts with the attachment of the mid-point of each cable to the bottom of the pile reinforcement cage, while the cage is lying horizontal, raised off the ground, using wooden blocks for example. The cables are then wrapped around half the diameter of the cage and anchored to the bottom of their respective sides (Figure 5a). This attachment can be by means of purpose-made cable clamps or by simply using plastic cable ties.

In single-cage piles, the cables can be installed ether on the inside or the outside of the pile cage. In the case of multi-cage piles, the cables are attached to the bottom-most cage only at first, and the cables have to be installed on the outside of the cage in order to allow

them to be unreeled along the subsequent cages while they are being inserted in the pile bore.

After being attached to the bottom of the reinforcement cage, the cables are then unreeled along each side of the cage. The remaining length of cable is left on the reels, which are tied temporarily to the top of the cage (Figure 5b). The cables should be held close to the reinforcement bars by means of loosely-tied cable ties along the length of the cage (Figure 5c). This ensures that the cables are not pushed outwards under the pressure of the concrete when the pile is being constructed, while allowing the cables to move longitudinally under strain.

When the instrumented cage is lifted and inserted into the pile bore, the cable reels are removed from the cage and, in the case of multi-cage piles, placed on cable reel stands (Figure 5d). As subsequent cages are joined and lowered in the bore, the cables are unreeled to descend into the bore along with the cages. Once all the cages have been lowered into the pile bore, the cables are anchored to the reinforcement at the pile head.
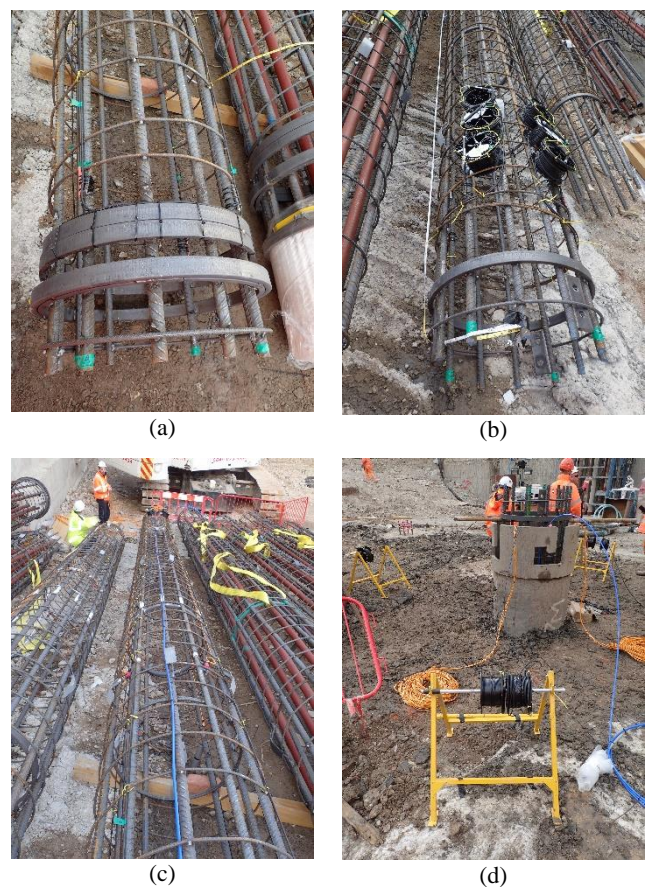

(a)

(b)

(c)

(d)

Figure 5 Stages of FO cables installation in the test pile used as a case study in Section 5: (a) FO cables anchored securely to the bottom of the bottom-most reinforcement cage, wrapped around the diameter of the cage and unreeled along the cage; (b) Remaining cables left on reels which are tied temporarily to the top of the bottom cage; (c) FO cables held to the outside of the cage by means of loose cable ties; (d) Cable reels placed on stands to be unwound as subsequent cages are lowered into the pile bore.

Before anchoring the strain cables, they should be stretched in order to apply pre-tension. In the case of compression piles, the amount of pretension should ideally be larger than the maximum amount of compressive strain that the pile is expected to undergo during the load test. This allows the compression strain to be measured as a reduction in cable pre-tension. However, the amount

of pre-tension applied to the strain cable should not exceed the elastic limit of the cable.

It is important to keep a record of the top and bottom anchor locations with respect to the length along the sensor cables, as well as the start and end of each sensor cable. One way of doing this is to record the chainage (distance along the cable), which is typically printed on the cable jacket at one metre intervals, that corresponds to the location of the anchor and to the start / end. This would enable the location of the sensing portion of cables to be identified along the length of the data vector obtained during monitoring (see Section 4).

The ends of the cables are brought out of the pile head, typically through a notch in the pile head casing, and connected together to form a complete circuit. The circuit is then connected to the FO spectrum analyser within the designated monitoring location, where the operating environment can be controlled to ensure the correct functioning of the analyser. Due to site constraints, the monitoring location is often not directly adjacent to the test pile, in which case either the sensing cables should be long enough to reach the analyser, or a FO extension cable can be used to connect the end of the sensing circuit to the analyser.

3.4 Integrity testing of the DFOS sensor system

The integrity of FO cables can be tested using a handheld optical time domain reflectometer (OTDR), which measures the attenuation rate along the length of an optical fibre and identifies the location of anomalies resulting in optical loss or reflectance. It is important to test the integrity of the DFOS cables at each stage of the installation, in order to identify any unexpected optical losses or damage to the optical fibre, which is often not visible from the outside, unless the cable has been completely cut through.

This testing should be done at least after the cables are installed on the bottom cage (while still on the ground), after the whole pile has been installed but before it is concreted (unless it is a CFA pile) and after the sensor cables are connected together. Typical causes of optical losses are sharp bends in the FO cable and dirty connectors, both of which can be rectified if detected in time. A break in an optical fibre is more difficult to rectify as it involves cutting off the damaged cable and fusion splicing the optical fibre back together.

4. DATA PROCESSING

The data obtained from the FO analyser consists of a vector of peak Brilloiun frequency recorded at each sampling point along the complete FO circuit. Before these data can be processed to obtain values of temperature and strain in the pile, the data vector needs to be related to the physical location of the cables within the pile.

Using the chainage records made during the installation, it is possible to obtain a close approximation to which parts of the data vector corresponds to which sensing location within the pile. This can be refined by visually inspecting the data and looking for features such as pre-strained sections of strain cables between anchoring points and temperature gradients where the cables exit the pile head. Figure 7 shows an example of this exercise carried out for the presented case study.

Once the sections of the data vector have been matched to their location in the pile, the temperature can be calculated from the temperature cable and subsequently the temperature-compensated axial mechanical strain can be calculated by combining Eq. 1 and Eq. 2:

$$\Delta\varepsilon_a = \frac{1}{C_\varepsilon}\left[\Delta v_{bS} - C_T \cdot \left(\frac{\Delta v_{bT}}{\beta}\right)\right] \tag{3}$$

Further post-processing may be performed based on the axial strain profiles obtained (Klar et al., 2006; Pelecanos et al., 2017; 2018). The geotechnical response of the pile may be assessed by determining the profiles of axial force, F_a, and vertical displacement, u, with the depth, z, respectively:

$$F_a(z) = EA \cdot \Delta\varepsilon_a(z) \tag{4}$$

$$u(z) = u(z = z_0) + \int_0^z \Delta\varepsilon_a(z)\,dz \tag{5}$$

where, EA is the axial rigidity of the pile as before and z is the depth from the top of the pile. For the vertical displacements, the relative displacements obtained from the integration of axial strain can be added to the measured absolute displacement values from displacement transducers at the pile head, where $z = z_0$.

5. CASE STUDY

The application of DFOS for pile testing is best illustrated by means of a case study. The project presented here was carried out in 2016 on a test pile in London, as part of the preliminary works for a mixed-use development comprising a number of towers, the tallest of which was to be 37 storeys high.

5.1 Test pile and load test details

The test pile was 0.9 m in diameter and 23 m long. The reinforcement consisted of two cages, each with 12 in number 32 mm-diameter steel bars and helical outer steel of 10 mm-diameter bars with a vertical pitch of 225 mm and an outer diameter of 0.75 m (Figure 6). The pile was constructed as a bored pile in a dry bore, without support fluid, excavated and concreted in a single shift.

The pile head extended approximately 0.4 m above the piling platform level, with a short steel sleeve (inner diameter 0.9 m) containing the above-ground part of the pile. The stratigraphy along the pile comprised made ground (backfill) up to a depth of around 4 m from the pile head, then London clay extending beyond the bottom of the pile, with a transition to a stiffer clay at a depth of 14.5 m below the pile head.
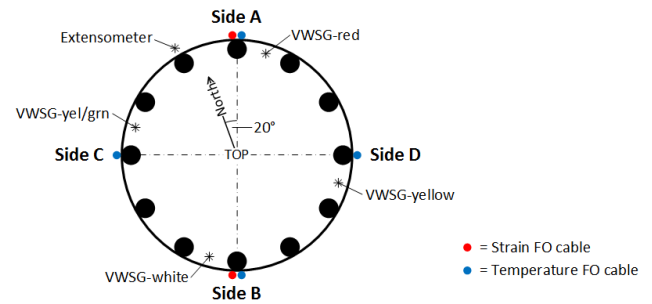

Figure 6 Cross-section of the pile cage showing the reinforcement and instrumentation positions (VWSG = vibrating wire strain gauge, FO = fibre optic).

The pile cage was instrumented with one loop of strain (single mode Fujikura 4-core 9.5/125 JBT-03813) and two loops of temperature (single mode loose-tube Excel 4-core 9/125 OS1) DFOS sensor cables. The FO cables were installed first on the bottom cage, then unreeled as the top cage was lowered into the pile bore, as described in Section 3 (Figure 5). In addition, traditional instrumentation was also installed in the pile. This consisted of 20 vibrating wire strain gauges (VWSGs) divided into sets of four gauges at five different levels, as well as one embedded rod extensometer to measure the overall change in length (relative displacement) between the pile head and toe.

The pile was load tested 43 days after it was concreted. The test consisted of a maintained compressive load applied in stages from a loading frame anchored to reaction piles, over three loading and unloading cycles. The maximum applied loads were 3.70 MN (100% DVL), 5.43 MN (100% DVL + 50% SWL) and 12.00 MN (100% DVL + 240% SWL) during the first, second and third load cycles, respectively.

Monitoring from the DFOS system was carried out throughout the load test using a Neubrescope NBX-5000 BOTDR Analyser manufactured by Neubrex, Japan. Measurements were recorded automatically once every 5 minutes, with a spatial resolution of 0.5 m, sampling interval of 0.05 m, and frequency step of 3 MHz. The data were divided into sections relating to each of the instrumented sides of the pile (Figure 7), before being processed to derive measurements of temperature and temperature-compensated strain, as explained in Section 4.
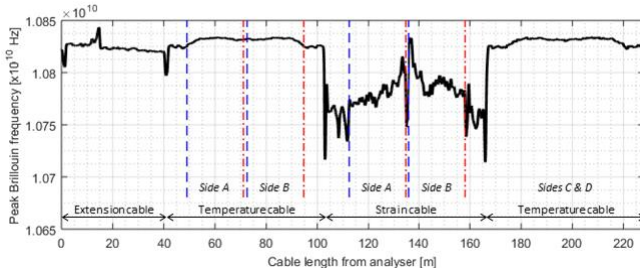

Figure 7 Baseline measurement taken from the DFOS system before the load test commenced, showing the sections of data relating to the physical location of the cables in the pile.

5.2   Results and discussion

The obtained Brillouin frequency data from the FO cables shown in Figure 7, were processed using Eq. 3 to obtain the relevant profiles of axial strain and selected such profiles are graphically shown in Figure 8 (a). It is shown that spatially continuous values of axial strain are available for the entire length of the pile, and these values increase with increasing load values. Continuous values of strain may indicate any areas of particular interest, such as strain localisation (Acikgoz et al., 2016; 2017). Further, numerical integration of the strain values with the depth, using Eq. 4, may provide the relevant profiles of vertical displacement along the depth of the pile. The latter is presented in Figure 8(b) which shows that there is consistent development of axial displacement with increasing load, which was expected, and which means that there is shortening of the pile as a result of the applied load and surrounding soil reaction.

Moreover, selected profiles of axial strain are shown in Figure 9. On the same figure the results of a simplified numerical finite element (FE) beam-spring model are included for comparison. The FE analysis assumed a single axially loaded pile modelled with linear beam elements and non-linear springs representing the surrounding soil. Global static equilibrium is satisfied according to:

$$[K_p + K_s] \cdot \{u\} = \{F\} \tag{6}$$

where, $[K_p]$ and $[K_s]$ are the global pile and soil stiffness matrices respectively, $\{u\}$ is the vector of the displacements and $\{F\}$ is the vector of the externally applied forces. The nonlinear soil spring is described by the Degradation and Hardening Hyperbolic Model (DHHM) model of Pelecanos & Soga (2017a, b):

$$t = \frac{k_m z}{\sqrt[d]{\left(1 + \left(\frac{k_m}{t_m}z\right)^{hd}\right)}} \tag{7}$$

where k_m is the maximum stiffness, t_m is the maximum value of shear stress, and d and h are the dimensionless degradation and hardening parameters. The values of the four model parameters are obtained by matching the axial strain, $\varepsilon_a(z)$, profiles resulting from the numerical model and those obtained from the DFOS measurements, as shown in Figure 9. More details about this approach are provided by Pelecanos & Soga (2017a, 2017b, 2018).

Three soil layers, represented by constant soil spring properties along the depth of each layer, were assumed following the local soil stratigraphy. The relevant model parameters adopted are listed in Table 1.

Table 1 Parameters of the FE model used

Layer	Depth [m]	k_m [MN/m³]	t_m [MN/m²]	d []	h []
1	0 – 4	30	0.3	1	1
2	4 – 14.5	200	0.4	1	1.55
3	14.5 – 23	300	0.35	1	1
Base	23	1560	6.3	1	1

Additional post-processing of the FO axial strains could involve differentiation to obtain shaft friction, F_s, profiles. However, the inherent waviness of the FO strains makes such differentiation cumbersome and therefore the values of F_s were instead obtained from the FE model (Pelecanos et al., 2018). The calculated strains from the model were in good agreement with the observed ones (Figure 9) and therefore the model was considered reliable for providing the relevant values of F_s.
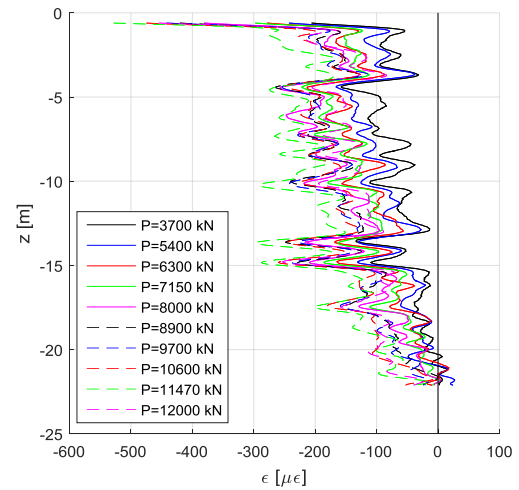
(a)
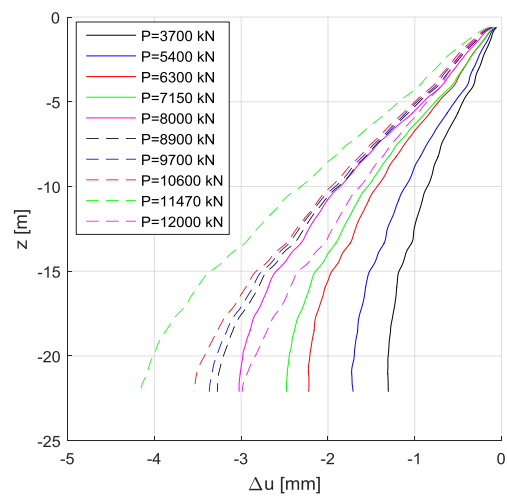
(b)

Figure 8 Observed FO data: (a) profiles of axial pile strains, (b) profiles of (relative) change in vertical displacement.
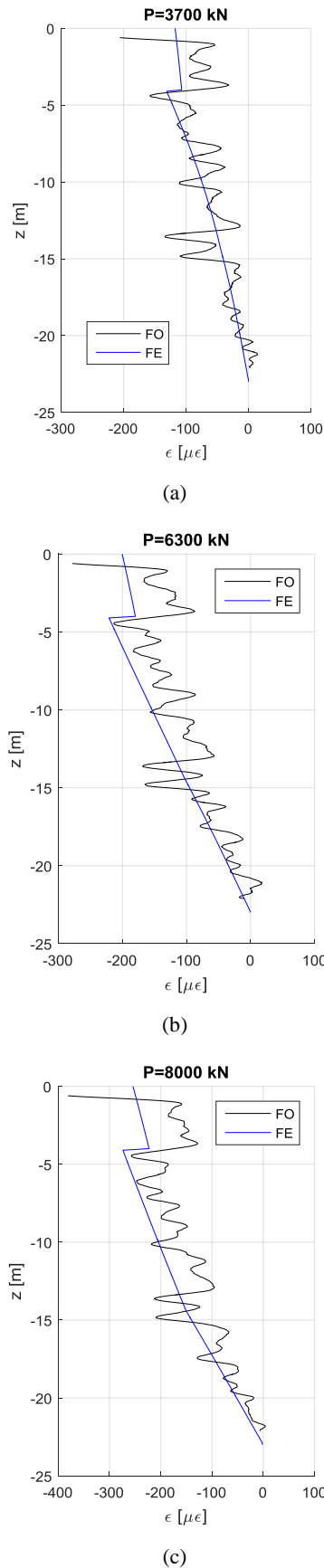
(a)

(b)

(c)

Figure 9 Profiles of observed (FO) and calculated (FE) axial strain for: (a) P=3700 kN, (b) P=6300 kN, (c) P=8000 kN

Figure 10 (a) and (b) show the obtained profiles of axial force and shaft friction, respectively, as calculated from the FE model. It is shown that there are smooth profiles of axial force, as expected, the slopes of which are related to the resistance of the surrounding soil. In addition, shaft friction profiles show that soil friction increases with the applied load, as larger resistance is mobilised. Also, as expected, larger soil resistance develops deeper in the ground, which should be due to the larger confining stress and therefore stiffness of the soil.
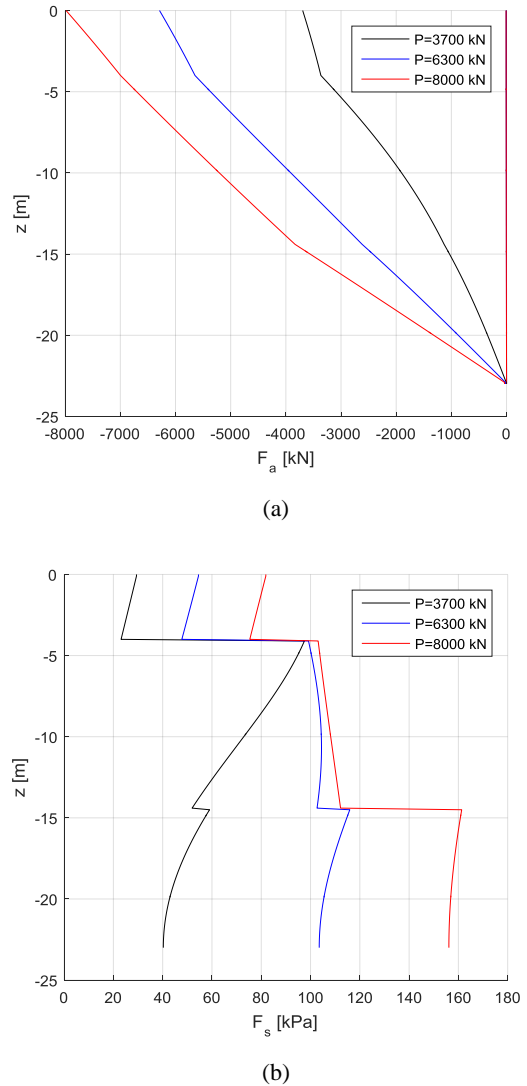

(a)

(b)

Figure 10 Profiles of computed pile response using the FE model: (a) axial pile forces, (b) shaft friction

6.   CONCLUSION

Pile load testing is a common procedure used by geotechnical engineers to guide the design of pile foundations of major projects. While concrete pile testing is an expensive part of a project's preliminary works, when the test piles are instrumented with the right sensor systems the load test can provide valuable information that can lead to an economical foundation design for the project. However, traditional instrumentation, typically consisting of embedded vibrating wire strain gauges (VWSGs) and extensometers, can only provide measurements at point locations within the pile. In this paper, the measurement of distributed strain along the entire length of the pile has been demonstrated. This was done using a distributed fibre optic sensor (DFOS) system based on the Brillouin scattering measurement technique.

The monitoring principles were described, as well as the basic steps involved in designing, installing, testing and measuring from the DFOS system in test piles. Through a case study of a bored pile instrumented and load tested in London in 2016, it has been shown how a DFOS system can provide data that are much more spatially dense than can be achieved with traditional instrumentation. This greatly reduces the uncertainties in measurements, as one no longer needs to assume a constant change of strain between point measurements, as is commonly done when piles are instrumented with VWSGs.

The pile under consideration was axially loaded from the top and was constantly monitored. The FO sensing cables provided a wealth of relevant axial pile strain data. The observed distributed strain profiles revealed the actual deformation of the pile which was smooth, as expected, and with no signs of any localised strain or any suggestions of pile damage. Integration of the strain values allowed the determination of the vertical displacements, which also revealed some noticeable axial shortening of the pile, a typical feature of such friction piles.

The observed performance of the pile was complemented by a relevant one-dimensional finite element analysis which provided further insight into the mobilised mechanism of pile-soil interaction. A good match between the FO observed and FE predicted strains provided a calibrated FE model which was used to obtain the relevant profiles of axial pile force and shaft friction. The latter two quantities were crucial in assessing the actual geotechnical behaviour of the pile and suggested that the observed smooth axial force profiles revealed a healthy pile with no signs of damage or localisation.

Finally, the inferred values of shaft friction confirmed the hypothesis of stiffer and stronger soil deeper in the ground and closer to the base of the pile, which is the typical behaviour of London Clay.

Overall, this study showed that DFOS can be used in routine pile design and construction and can provide a wealth of relevant information that can assist both the pile designer and contractor in ensuring that high quality assurance of the constructed piles is maintained and controlled.

7. ACKNOWLEDGEMENTS

8. REFERENCES

Acikgoz, M. S., Pelecanos, L., Giardina, G., Aitken, J. and Soga, K., 2016. "Field monitoring of piling effects on a nearby masonry vault using distributed sensing", International Conference on Smart Infrastructure and Construction (ICSIC), ICE Publishing, Cambridge, UK

Acikgoz, M. S., Pelecanos, L., Giardina, G., Aitken, J. and Soga, K., 2017. "Distributed sensing of a masonry vault due to nearby piling". Structural Control and Health Monitoring, 24 (3), e1872.

Bao, X., Chen, L. 2011. "Recent progress in Brillouin scattering based fiber sensors", Sensors, 11, pp 4152-4187.

Bennett, P. J., Klar, A., Vorster, T. E. B., Choy, C. K., Mohamad, H., Soga, K., Mair, R. J., Tester, P. D., and Fernie, R. 2006. "Distributed Optical Fibre Strain Sensing in Piles", in A. P. Butcher, J. J. M. Powell, and H. D. Skinner (eds.), Reuse of Foundations for Urban Sites: Proceedings of International Conference, volume EP73, pp. 105-114, Watford, UK. IHS BRE Press.

British Standards Institution, 2004. BS EN 1997-1:2004+A1:2013 Eurocode 7. Geotechnical design. General rules, London, UK: BSI.

de Battista, N., Kechavarzi, C. and Soga, K. 2016a. "Distributed fiber optic sensors for monitoring reinforced concrete piles using Brillouin scattering", in Proceedings of the European Workshop on Optical Fibre Sensors - EWOFS 2016. Limerick, Ireland: SPIE.

de Battista, N., Kechavarzi, C., Seo, H., Soga, K. and Pennington, S. 2016b. "Distributed fibre optic sensors for measuring strain and temperature of cast-in-situ concrete test piles", International Conference on Smart Infrastructure and Construction (ICSIC), ICE Publishing, Cambridge, UK, pp 21-26.

Federation of Piling Specialists, 2006. Handbook on pile load testing, Beckenham, Kent, UK: Federation of Piling Specialists.

Horiguchi, T.; Kurashima, T. and Tateda, M. 1989. Tensile strain dependence of Brillouin frequency shift in silica optical fibers. Photonics Technology Letters, 1(5), pp 107-108.

Institute of Civil Engineers 2017. "Specification for Piling and Embedded Retaining Walls", Third edition, ICE Publishing, London, UK, 248p. ISBN: 9780727760555

Kechavarzi, C., Soga, K., de Battista, N., Pelecanos, L., Elshafie, M.Z.E.B. and Mair, R.J. 2016. "Distributed Fibre Optic Strain Sensing for Monitoring Civil Infrastructure - A Practical Guide", ICE Publishing, London, UK, 264p. ISBN: 9780727760555

Klar, A., Bennett, P. J., Soga, K., Mair, R. J., Tester, P., Fernie, R., St John, H. D., and Torp-Peterson, G. 2006. "Distributed Strain Measurement for Pile Foundations", Proceedings of the Institution of Civil Engineers - Geotechnical Engineering, 159, pp 135-144.

Ouyang, Y., Broadbent, K., Bell, A., Pelecanos, L. and Soga, K., 2015. "The use of fibre optic instrumentation to monitor the O-Cell load test on a single working pile in London", XVI European Conference on Soil Mechanics and Geotechnical Engineering, 2015-09-13 - 2015-09-17.

Pelecanos, L. and Soga, K. 2017a. "Innovative Structural Health Monitoring Of Foundation Piles Using Distributed Fibre-Optic Sensing", 8th International Conference on Structural Engineering and Construction Management 2017, Kandy, Sri Lanka, 7/12/17 - 10/12/17, pp. 1-8.

Pelecanos, L. and Soga, K. 2017b. "The use of distributed fibre-optic strain data to develop finite element models for foundation piles", 6th International Forum on Opto-electronic Sensor-based Monitoring in Geo-engineering, Nanjing, China, 3/11/17, pp. 1-9.

Pelecanos, L., Soga, K., Hardy, S., Blair, A., and Carter, K. 2016. "Distributed fibre optic monitoring of tension piles under a basement excavation at the V&A museum in London", International Conference on Smart Infrastructure and Construction (ICSIC), ICE Publishing, Cambridge, UK

Pelecanos, L., Soga, K., Chunge, M., Ouyang, Y., Kwan, V., Kechavarzi, C., Nicholson, D.P. 2017. "Distributed fibre-optic monitoring of an Osterberg-cell pile test in London", Geotechnique Letters, 7, pp 1-9.

Pelecanos, L., Soga, K., Elshafie, M., de Battista, N., Kechavarzi, C., Gue, C. Y., Ouyang, Y. and Seo, H. 2018. "Distributed Fibre Optic Sensing of Axially Loaded Bored Piles in Stiff Clay", Journal of Geotechnical and Geoenvironmental Engineering, ASCE, 144(3): 04017122.

Soga, K. 2014. XII Croce Lecture: "Understanding the real performance of geotechnical structures using an innovative fibre optic distributed strain measurement technology", Rivista Italiana di Geotechnica, 4, pp 7-48.

Soga, K., Kwan, V., Pelecanos, L., Rui, Y., Schwamb, T., Seo, H. and Wilcock, M., 2015. "The Role of Distributed Sensing in Understanding the Engineering Performance of Geotechnical Structures", XVI European Conference on Soil Mechanics and Geotechnical Engineering, 2015-09-13 - 2015-09-17.

Soga, K., Kechavarzi, C., Pelecanos, L., de Battista, N., Williamson, M., Gue, C. Y., Di Murro, V. and Elshafie, M. 2017. "Distributed fibre optic strain sensing for monitoring underground structures- Tunnels case studies.", Underground sensing, S. Pamukcu and L. Cheng, eds., 1st Ed., Elsevier, Amsterdam, Netherlands.

Zhang, H., Wu, Z. 2008. "Performance evaluation of BOTDR-based distributed fiber optic sensors for crack monitoring", Structural Health Monitoring, 7, pp 143-156.